CHAPTER 24

AIRFLOW AROUND BUILDINGS

AIRFLOW around buildings affects worker safety, process and building equipment operation, weather and pollution protection at inlets, and the ability to control indoor temperature, humidity, air motion, and contaminants. Wind causes variable surface pressures on buildings that change intake and exhaust system flow rates, natural ventilation, infiltration and exfiltration, and interior pressures. The mean flow patterns and turbulence of wind passing over a building can recirculate exhaust gases to air intakes. This chapter provides basic information for evaluating windflow patterns, estimating wind pressures, and identifying problems caused by the effects of wind on intakes, exhausts, and equipment. In most cases, detailed solutions are addressed in other chapters. Related information can be found in Chapters 11, 14, 16, and 36 of this volume; in Chapters 29, 30, 44, 46, and 52 of the 2007 *ASHRAE Handbook—HVAC Applications*; and in Chapters 29, 34, and 39 of the 2008 *ASHRAE Handbook—HVAC Systems and Equipment*.

FLOW PATTERNS

Buildings having even moderately complex shapes, such as L- or U-shaped structures, can generate flow patterns too complex to generalize for design. To determine flow conditions influenced by surrounding buildings or topography, wind tunnel or water channel tests of physical scale models, tests of existing buildings, or careful computational modeling efforts are required (see the section on Physical and Computational Modeling). Only isolated, rectangular block buildings are discussed here. English and Fricke (1997), Hosker (1984, 1985), Khanduri et al. (1998), Saunders and Melbourne (1979), and Walker et al. (1996) review the effects of nearby buildings.

As wind impinges on a building, airflow separates at the building edges, generating recirculation zones over downwind surfaces (roof, side and downwind walls) and extending into the downwind wake (Figure 1). On the upwind wall, surface flow patterns are largely influenced by approach wind characteristics. Figure 1 shows that the mean speed of wind U_H approaching a building increases with height H above the ground. Higher wind speed at roof level causes a larger pressure on the upper part of the wall than near the ground, which leads to **downwash** on the lower one-half to two-thirds of the building. On the upper one-quarter to one-third of the building, windflow is directed upward over the roof (**upwash**). For a building with height H three or more times width W of the upwind face, an intermediate stagnation zone can exist between the upwash and downwash regions, where surface streamlines pass horizontally around the building, as shown in Figures 1 (inset) and 2. (In Figure 2, the upwind building surface is "folded out" to illustrate upwash, downwash, and stagnation zones.) Downwash on the lower surface of the upwind face separates from the building before it reaches ground level and moves upwind to form a vortex that can generate high velocities close to the ground ("area of strong surface wind" in

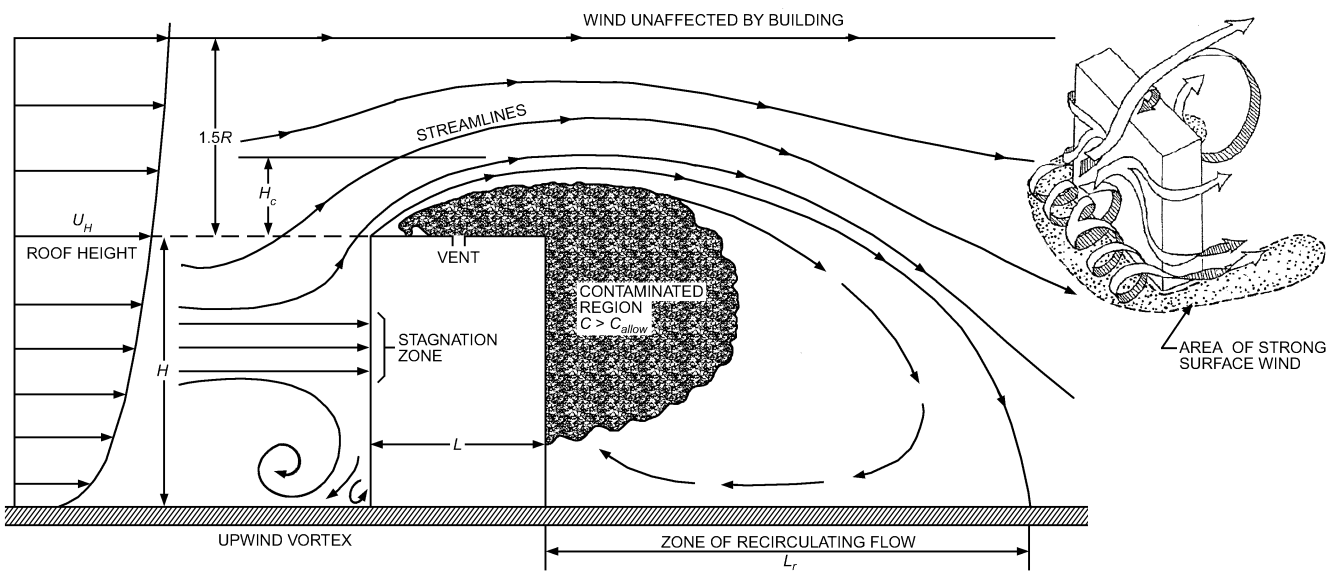

Fig. 1 Flow Patterns Around Rectangular Building

The preparation of this chapter is assigned to TC 4.3, Ventilation Requirements and Infiltration.

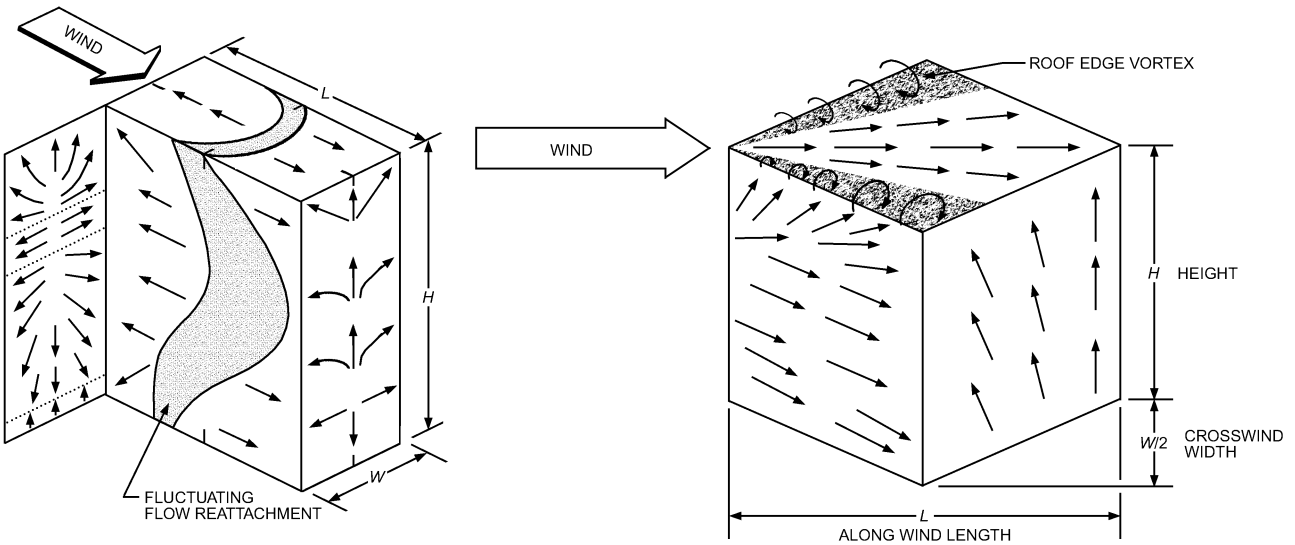

Fig. 2 Surface Flow Patterns for Normal and Oblique Winds
(Wilson 1979)

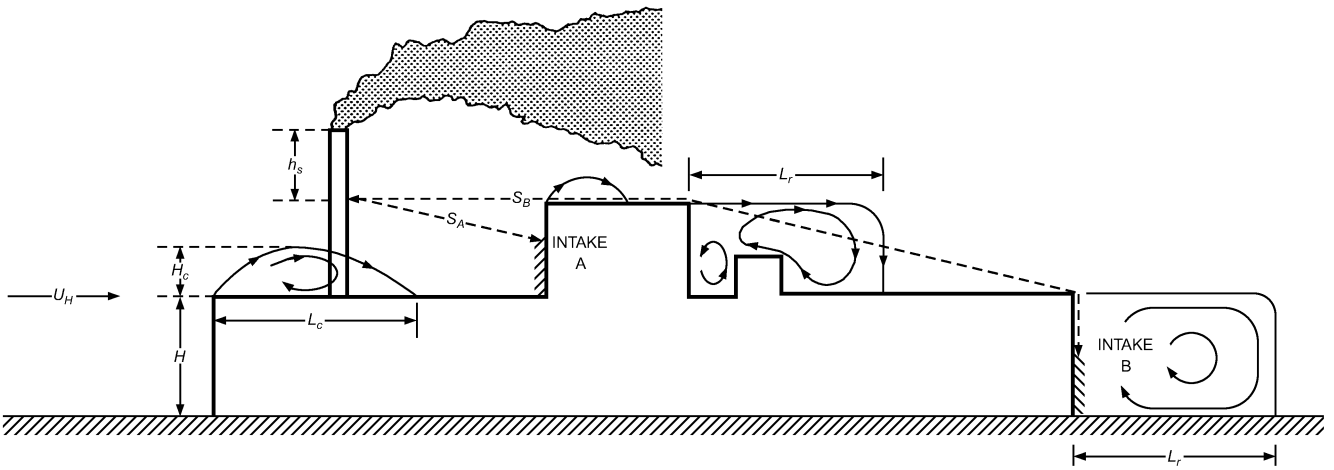

Fig. 3 Flow Recirculation Regions and Exhaust-to-Intake Stretched-String Distances (S_A, S_B)

Figure 1, inset). This ground-level upwind vortex is carried around the sides of the building in U shape and suspends dust and debris that can contaminate air intakes close to ground level.

The downwind wall of a building exhibits a region of low average velocity and high turbulence (i.e., a **flow recirculation** region) extending a distance L_r downwind. If the building has sufficient length L in the windward direction, the flow reattaches to the building and may generate two distinct regions of separated recirculation flow, on the building and in its wake, as shown in Figures 2 and 3. Figure 3 also illustrates a rooftop recirculation cavity of length L_c at the upwind roof edge and a recirculation zone of length L_r downwind of the rooftop penthouse. Velocities near the downwind wall are typically one-quarter of those at the corresponding upwind wall location. Figures 1 and 2 show that an upward flow exists over most of the downwind walls.

Streamline patterns are independent of wind speed and depend mainly on building shape and upwind conditions. Because of the three-dimensional flow around a building, the shape and size of the recirculation airflow are not constant over the surface. Airflow reattaches closer to the upwind building face along the edges of the building than it does near the middle of the roof and sidewalls (Figure 2). Recirculation cavity height H_c (Figures 1 and 3) also decreases near roof edges. Calculating characteristic dimensions for recirculation zones H_c, L_c, and L_r is discussed in Chapter 44 of the 2007 *ASHRAE Handbook—HVAC Applications*.

For wind perpendicular to a building wall, height H and width W of the upwind building face determine the **scaling length** R that characterizes the building's influence on windflow. According to Wilson (1979),

$$R = B_s^{0.67} B_L^{0.33} \quad (1)$$

where

B_s = smaller of upwind building face dimensions H and W
B_L = larger of upwind building face dimensions H and W

When B_L is larger than $8B_s$, use $B_L = 8B_s$ in Equation (1). For buildings with varying roof levels or with wings separated by at least a distance of B_s, only the height and width of the building face below the portion of the roof in question should be used to calculate R.

Flow accelerates as the streamlines compress over the roof and decelerates as they spread downward over the wake on the downwind side of the building. The distance above roof level where a building influences the flow is approximately 1.5R, as shown in

Figure 1. In addition, roof pitch also begins to affect flow when it exceeds about 15° (1:4). When roof pitch reaches 20° (1:3), flow remains attached to the upwind pitched roof and produces a recirculation region downwind of the roof ridge that is larger than that for a flat roof.

If the angle of the approach wind is not perpendicular to the upwind face, complex flow patterns result. Strong vortices develop from the upwind edges of a roof, causing strong downwash onto the roof (Figure 2). High speeds in these vortices (vorticity) cause large negative pressures near roof corners that can be a hazard to roof-mounted equipment during high winds. When the angle between the wind direction and the upwind face of the building is less than about 70°, the upwash/downwash patterns on the upwind face of the building are less pronounced, as is the ground-level vortex shown in Figure 1. Figure 2 shows that, for an approach flow angle of 45°, streamlines remain close to the horizontal in their passage around the sides of the building, except near roof level, where the flow is sucked upward into the roof edge vortices (Cochran 1992).

Both the upwind velocity profile shape and its turbulence intensity strongly influence flow patterns and surface pressures (Melbourne 1979).

WIND PRESSURE ON BUILDINGS

In addition to flow patterns described previously, the turbulence or gustiness of approaching wind and the unsteady character of separated flows cause surface pressures to fluctuate. Pressures discussed here are time-averaged values, with an averaging period of about 600 s. This is approximately the shortest time period considered to be a "steady-state" condition when considering atmospheric winds; the longest is typically 3600 s. Instantaneous pressures may vary significantly above and below these averages, and peak pressures two or three times the mean values are possible. Although peak pressures are important with regard to structural loads, mean values are more appropriate for computing infiltration and ventilation rates. Time-averaged surface pressures are proportional to wind velocity pressure p_v given by Bernoulli's equation:

$$p_v = \frac{\rho_a U_H^2}{2 g_c} \tag{2}$$

where

U_H = approach wind speed at upwind wall height H [see Equation (4)]
ρ_a = ambient (outdoor) air density
g_c = gravitational proportionality constant

The proportional relationship is shown in the following equation, in which the difference p_s between the pressure on the building surface and the local outdoor atmospheric pressure at the same level in an undisturbed wind approaching the building is

$$p_s = C_p p_v \tag{3}$$

where C_p is the local wind pressure coefficient at a point on the building surface.

The local wind speed U_H at the top of the wall that is required for Equation (2) is estimated by applying terrain and height corrections to the hourly wind speed U_{met} from a nearby meteorological station.

U_{met} is generally measured in flat, open terrain (i.e., category 3 in Table 1). The anemometer that records U_{met} is located at height H_{met}, usually 33 ft above ground level. The hourly average wind speed U_H (Figures 1 and 3) in the undisturbed wind approaching a building in its local terrain can be calculated from U_{met} as follows:

$$U_H = U_{met}\left(\frac{\delta_{met}}{H_{met}}\right)^{a_{met}}\left(\frac{H}{\delta}\right)^{a} \tag{4}$$

Table 1 Atmospheric Boundary Layer Parameters

Terrain Category	Description	Exponent a	Layer Thickness δ, ft
1	Large city centers, in which at least 50% of buildings are higher than 80 ft, over a distance of at least 0.5 mi or 10 times the height of the structure upwind, whichever is greater	0.33	1500
2	Urban and suburban areas, wooded areas, or other terrain with numerous closely spaced obstructions having the size of single-family dwellings or larger, over a distance of at least 0.5 mi or 10 times the height of the structure upwind, whichever is greater	0.22	1200
3	Open terrain with scattered obstructions having heights generally less than 30 ft, including flat open country typical of meteorological station surroundings	0.14	900
4	Flat, unobstructed areas exposed to wind flowing over water for at least 1 mi, over a distance of 1500 ft or 10 times the height of the structure inland, whichever is greater	0.10	700

The atmospheric boundary layer thickness δ and exponent a for the local building terrain and a_{met} and δ_{met} for the meteorological station are determined from Table 1. Typical values for meteorological stations (category 3 in Table 1) are $a_{met} = 0.14$ and $\delta_{met} = 900$ ft. The values and terrain categories in Table 1 are consistent with those adopted in other engineering applications (e.g., ASCE *Standard* 7). Equation (4) gives the wind speed at height H above the average height of local obstacles, such as buildings and vegetation, weighted by the plan-area. At heights at or below this average obstacle height (e.g., at roof height in densely built-up suburbs), speed depends on the geometrical arrangement of the buildings, and Equation (4) is less reliable.

An alternative mathematical description of the atmospheric boundary layer, which uses a logarithmic function, is given by Deaves and Harris (1978). Although their model is more complicated than the power law used in Equation (4), it more closely models the real physics of the atmosphere and has been adopted by several foreign codes (e.g., SA/SNZ *Standard* AS/NZS 1170.2 from Australia).

Example 1. Assuming a 23 mph anemometer wind speed for a height H_{met} of 33 ft at a nearby airport, determine the wind speed U_H at roof level $H = 50$ ft for a building located in a city suburb.

Solution: From Table 1, the atmospheric boundary layer properties for the anemometer are $a_{met} = 0.14$ and $\delta_{met} = 900$ ft. The atmospheric boundary layer properties at the building site are $a = 0.22$ and $\delta = 1200$ ft. Using Equation (4), wind speed U_H at 50 ft is

$$U_H = 23\left(\frac{900}{33}\right)^{0.14}\left(\frac{50}{1200}\right)^{0.22} = 18.2 \text{ mph}$$

Local Wind Pressure Coefficients

Values of the mean local wind pressure coefficient C_p used in Equation (3) depend on building shape, wind direction, and influence of nearby buildings, vegetation, and terrain features. Accurate determination of C_p can be obtained only from wind tunnel model tests of the specific site and building or full-scale tests. Ventilation rate calculations for single, unshielded rectangular buildings can be reasonably estimated using existing wind tunnel data. Many wind load codes (e.g., ASCE *Standard* ASCE/SEI 7-05, SA/SNZ *Standard* AS/NZS 1170.2) give mean pressure coefficients for common building shapes.

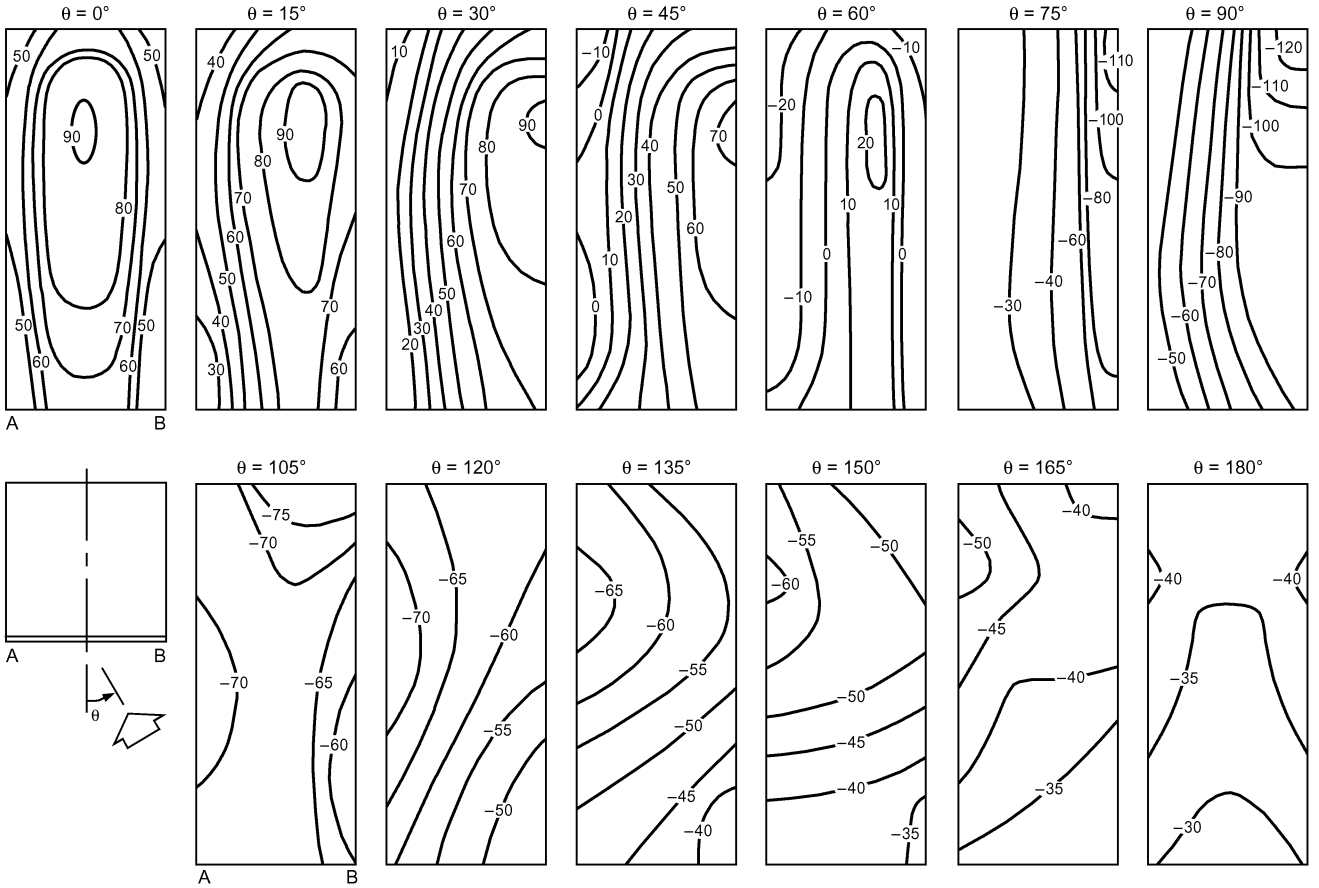

Fig. 4 Local Pressure Coefficients ($C_p \times 100$) for Tall Building with Varying Wind Direction
(Davenport and Hui 1982)

Figure 4 shows pressure coefficients for walls of a tall rectangular cross section building (high-rise) sited in urban terrain (Davenport and Hui 1982). Figure 5 shows pressure coefficients for walls of a low-rise building (Holmes 1986). Generally, for high-rise buildings, height H is more than three times the crosswind width W. For $H > 3W$, use Figure 4; for $H < 3W$, use Figure 5. At a wind angle $\theta = 0°$ (e.g., wind perpendicular to the face in question), pressure coefficients are positive, and their magnitudes decrease near the sides and the top as flow velocities increase.

As seen in Figure 4, C_p generally increases with height, which reflects increasing velocity pressure in the approach flow as wind speed increases with height. As wind direction moves off normal ($\theta = 0°$), the region of maximum pressure occurs closer to the upwind edge (B in Figure 4) of the building. At a wind angle of $\theta = 45°$, pressures become negative at the downwind edge (A in Figure 4) of the front face. At some angle θ between 60° and 75°, pressures become negative over the whole front face. For $\theta = 90°$, maximum suction (negative) pressure occurs near the upwind edge (B in Figure 4) of the building side and then recovers towards a lower-magnitude negative coefficient as the downwind edge (A in Figure 4) is approached. The degree of this recovery depends on the length of the side in relation to the width W of the structure. For wind angles larger than $\theta = 100°$, the side is completely within the separated flow of the wake and spatial variations in pressure over the face are not as great. The average pressure on a face is positive for wind angles from $\theta = 0°$ to almost 60° and negative (suction) for $\theta = 60°$ to 180°.

A similar pattern of behavior in wall pressure coefficients for a low-rise building is shown in Figure 5. Here, recovery from strong suction with distance from the upwind edge is more rapid.

Surface-Averaged Wall Pressures

Surface-averaged pressure coefficients may be used to determine ventilation and/or infiltration rates, as discussed in Chapter 16. Figure 6 shows the surface pressure coefficient C_s averaged over a complete wall of a low-rise building (Swami and Chandra 1987). The figure also includes values calculated from pressure distributions in Figure 5. Similar results for a tall building are shown in Figure 7 (Akins et al. 1979).

The wind-induced indoor/outdoor pressure difference is found using the coefficient $C_{p\,(in\text{-}out)}$, which is defined as

$$C_{p\,(in\text{-}out)} = C_p - C_{in} \tag{5}$$

where C_{in} is the internal wind-induced pressure coefficient. For uniformly distributed air leakage sites in all the walls, C_{in} is about –0.2, as can be found easily by integration.

Roof Pressures

Surface pressures on the roof of a low-rise building depend strongly on roof slope. Figure 8 shows typical distributions for a wind direction normal to a side of the building. Note that the direction and magnitude of pressure coefficients are indicated by the direction and length of the arrows. For very low slopes (less than about 10°), pressures are negative over the whole roof surface. The magnitude is greatest within the separated flow zone near the leading edge and recovers toward the free stream pressure downwind of the edge. For intermediate slopes (about 10 to 20°), two large-magnitude low-pressure regions are formed, one at the leading roof edge and one at the roof peak. For steeper slopes (greater than about 20°), pressures are weakly positive on the upwind slope and

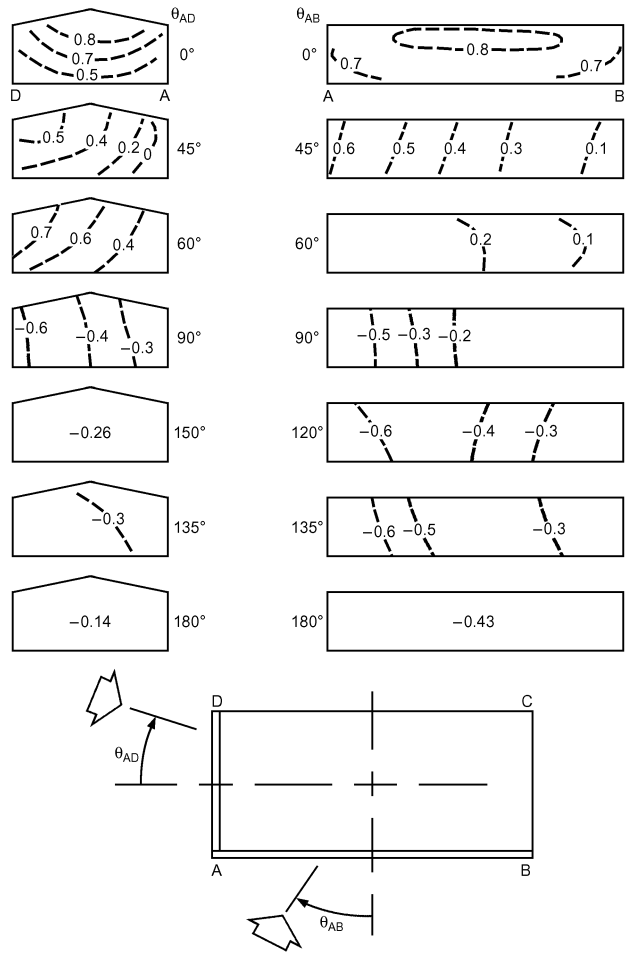

Fig. 5 Local Pressure Coefficients for Walls of Low-Rise Building with Varying Wind Direction

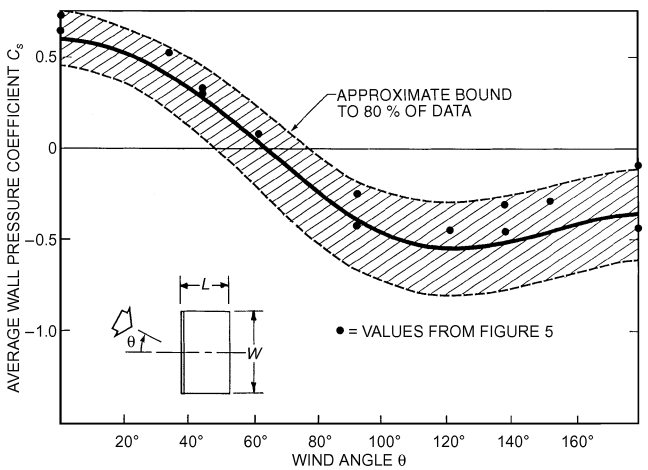

Fig. 6 Variation of Surface-Averaged Wall Pressure Coefficients for Low-Rise Buildings

Courtesy of Florida Solar Energy Center
(Swami and Chandra 1987)

negative within the separated flow over the downwind slope. With a wind angle of about 45°, the vortices originating at the leading corner of a roof with a low slope can induce very large, localized negative pressures (see Figure 2). A similar vortex forms on the

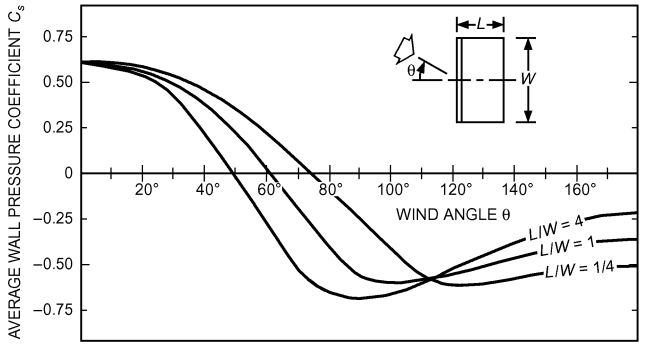

Fig. 7 Surface-Averaged Wall Pressure Coefficients for Tall Buildings

(Akins et al. 1979)

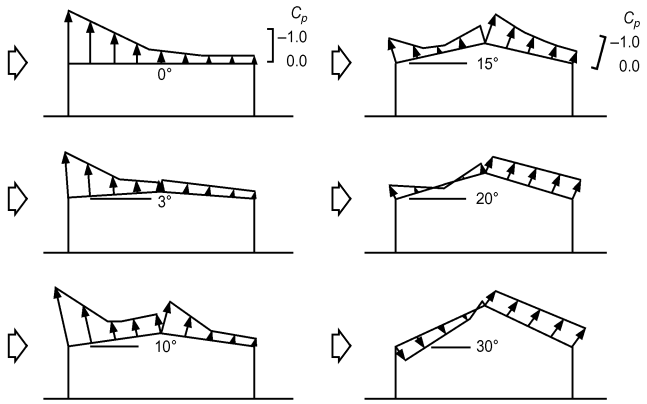

Fig. 8 Local Roof Pressure Coefficients for Roof of Low-Rise Buildings

(Holmes 1983)

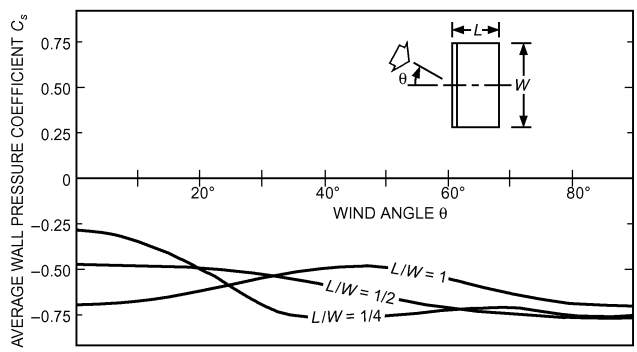

Fig. 9 Surface-Averaged Roof Pressure Coefficients for Tall Buildings

(Akins et al. 1979)

downwind side of a leading ridge end on a steep roof, as discussed in Cochran et al. (1999). Roof corner vortices and how to disrupt their influence are discussed in Cochran and Cermak (1992) and Cochran and English (1997). Figure 9 shows the average pressure coefficient over the roof of a tall building (Akins et al. 1979).

Interference and Shielding Effects on Pressures

Nearby structures strongly influence surface pressures on both high- and low-rise buildings, particularly for spacing-to-height ratios less than five, where distributions of pressure shown in Figures 4 to 9 do not apply. Although the effect of shielding for low-rise buildings is still significant at larger spacing, it is largely accounted

for by the reduction in p_v with increased terrain roughness. Bailey and Kwok (1985), Khanduri et al. (1998), Saunders and Melbourne (1979), Sherman and Grimsrud (1980), and Walker et al. (1996) discuss interference. English and Fricke (1997) discuss shielding through use of an interference index, and Walker et al. (1996) present a wind shadow model for predicting shelter factors. Chapter 16 gives shielding classes for air infiltration and ventilation applications.

Sources of Wind Data

To design for effects of airflow around buildings, wind speed and direction frequency data are necessary. The simplest forms of wind data are tables or charts of climatic normals, which give hourly average wind speeds, prevailing wind directions, and peak gust wind speeds for each month. This information can be found in sources such as *The Weather Almanac* (Bair 1992) and the *Climatic Atlas of the United States* (DOC 1968). Climatic design information, including wind speed at various frequencies of occurrence, is included in Chapter 14. A current source, which contains information on wind speed and direction frequencies, is the *International Station Meteorological Climatic Summary* CD from the National Climatic Data Center (NCDC) in Asheville, NC. Where more detailed information is required, digital records of hourly winds and other meteorological parameters are available (on magnetic tape or CD-ROM) from the NCDC for stations throughout the world. Most countries also have weather services that provide data. For example, in Canada, the Atmospheric Environment Service in Downsview, Ontario, provides hourly meteorological data and summaries.

When an hourly wind speed U_{met} at a specified probability level (e.g., the wind speed that is exceeded 1% of the time) is desired, but only the average annual wind speed U_{annual} is available for a given meteorological station, U_{met} may be estimated from Table 2. The ratios U_{met}/U_{annual} are based on long-term data from 24 weather stations widely distributed over North America. At these stations, U_{annual} ranges from 7 to 14 mph The uncertainty ranges listed in Table 2 are one standard deviation of the wind speed ratios. The following example demonstrates the use of Table 2.

Example 2. The wind speed U_{met} that is exceeded 1% of the time (88 hours per year) is needed for a building pressure or exhaust dilution calculation. If $U_{annual} = 9$ mph, find U_{met}.

Solution: From Table 2, the wind speed U_{met} exceeded 1% of the time is 2.5 ± 0.4 times U_{annual}. For $U_{annual} = 9$ mph, U_{met} is 23 mph with an uncertainty range of 19 to 26 mph at one standard deviation.

Using a single prevailing wind direction for design can cause serious errors. For any set of wind direction frequencies, one direction always has a somewhat higher frequency of occurrence. Thus, it is often called the **prevailing wind**, even though winds from other directions may be almost as frequent.

When using long-term meteorological records, check the anemometer location history, because the instrument may have been relocated and its height varied. This can affect its directional exposure and the recorded wind speeds. Equation (4) can be used to correct wind data collected at different mounting heights. Poor anemometer exposure caused by obstructions or mounting on top of a building cannot be easily corrected, and records for that period should be deleted.

If an estimate of the probability of an extreme wind speed outside the range of the recorded values at a site is required, the observations may be fit to an appropriate probability distribution (e.g., a Weibull distribution) and the particular probabilities calculated from the resulting function (Figure 10). This process is usually repeated for each of 16 wind directions (e.g., 22.5° intervals). Note that most recent wind data records are provided in 10° intervals, for which the same method may be used, except that the process is repeated for each of 36 wind directions. If both types of data are to be used, one data set must be transformed to match the other.

Where estimates at extremely low probability (high wind speed) are required, curve fitting at the tail of the probability distribution is very important and may require special statistical techniques applicable to extreme values (see Chapter 14). Building codes for wind loading on structures contain information on estimating extreme wind conditions. For ventilation applications, extreme winds are usually not required, and the 99 percentile limit can be accurately estimated from airport data averaged over less than 10 years.

Table 2 Typical Relationship of Hourly Wind Speed U_{met} to Annual Average Wind Speed U_{annual}

Percentage of Hourly Values That Exceed U_{met}	Wind Speed Ratio U_{met}/U_{annual}
90%	0.2 ± 0.1
75%	0.5 ± 0.1
50%	0.8 ± 0.1
25%	1.2 ± 0.15
10%	1.6 ± 0.2
5%	1.9 ± 0.3
1%	2.5 ± 0.4

Estimating Wind at Sites Remote from Recording Stations

Many building sites are located far from the nearest long-term wind recording site, which is usually an airport meteorological station. To estimate wind conditions at such sites, the terrain surrounding both the anemometer site and the building site should be checked. In the simplest case of flat or slightly undulating terrain

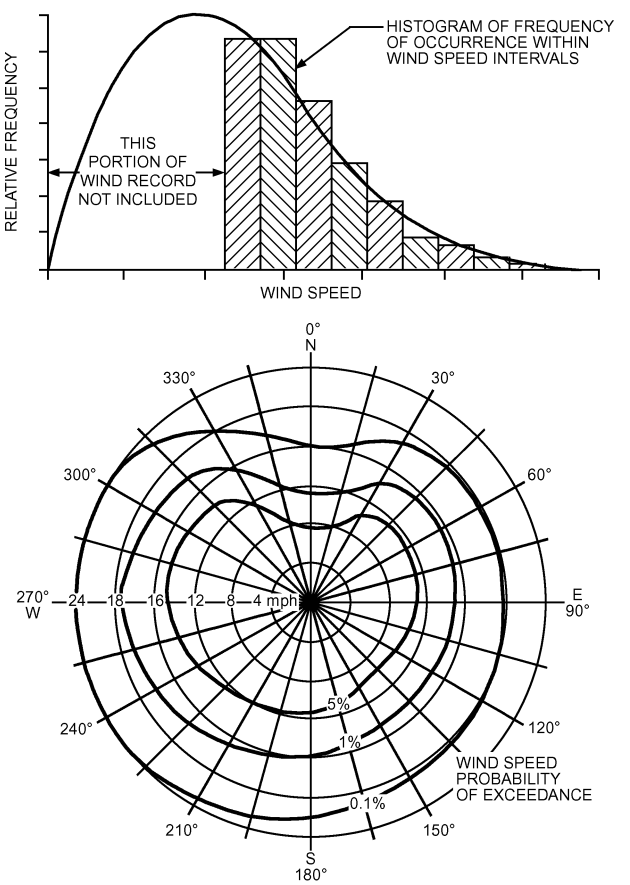

Fig. 10 Frequency Distribution of Wind Speed and Direction

with few obstructions extending for large distances around and between the anemometer site and building site, recorded wind data can be assumed to be representative of that at the building site. Wind direction occurrence frequency at a building site should be inferred from airport data only if the two locations are on the same terrain, with no terrain features that could alter wind direction between them.

In cases where the only significant difference between the anemometer site terrain and the building site terrain is surface roughness, the mean wind speed can be adjusted using Equation (4) and Table 1, to yield approximate wind velocities at the building site. Wind direction frequencies at the site are assumed to be the same as at the recording station.

In using Equation (4), cases may be encountered where, for a given wind direction, the terrain upwind of either the building or recording site does not fall into just one of the categories in Table 1. The terrain immediately upwind of the site may fall into one category, while that somewhat further upwind falls into a different category. For example, at a downtown airport the terrain may be flat and open (category 3) immediately around the recording instrument, but urban or suburban (category 2) a relatively short distance away. This difference in terrains also occurs when a building or recording site is in an urban area near open water or at the edge of town. In these cases, the suggested approach is to use the terrain category most representative of the average condition within approximately 1 mile upwind of the site (Deaves 1981). If the average condition is somewhere between two categories described in Table 1, the values of a and δ can be interpolated from those given in the table.

Several other factors are important in causing wind speed and direction at a building site to differ from values recorded at a nearby meteorological station. Wind speeds for buildings on hillcrests or in valleys where the wind is accelerated or channeled can be 1.5 times higher than meteorological station data. Wind speeds for buildings sheltered in the lee of hills and escarpments can be reduced to 0.5 times the values at nearby flat meteorological station terrain.

Solar heating of valley slopes can cause light winds of 2 to 9 mph to occur as warm air flows upslope. At night, radiant cooling of the ground can produce similar speeds as cold air drains downslope. In general, rolling terrain experiences a smaller fraction of low speeds than nearly flat terrain.

When wind is calm or light in the rural area surrounding a city, urban air tends to rise in a buoyant plume over the city center. This rising air, heated by anthropogenic sources and higher solar absorption in the city, is replaced by air pushed toward the city center from the edges. In this way, the urban heat island can produce light wind speeds and direction frequencies significantly different than those at a rural meteorological station.

In more complex terrain, both wind speed and direction may be significantly different from those at the distant recording site. In these cases, building site wind conditions should not be estimated from airport data. Options are either to establish an on-site wind recording station or to commission a detailed wind tunnel correlation study between the building site and long-term meteorological station wind observations.

WIND EFFECTS ON SYSTEM OPERATION

A building with only upwind openings is under a positive pressure (Figure 11A). Building pressures are negative when there are only downwind openings (Figure 11B). A building with internal partitions and openings (Figure 11C) is under various pressures, depending on the relative sizes of openings and wind direction. With larger openings on the upwind face, the building interior tends toward positive pressure; the reverse is also true (see Figures 4 to 9, and Chapter 16).

With few exceptions, building intakes and exhausts cannot be located or oriented such that a prevailing wind ensures ventilation

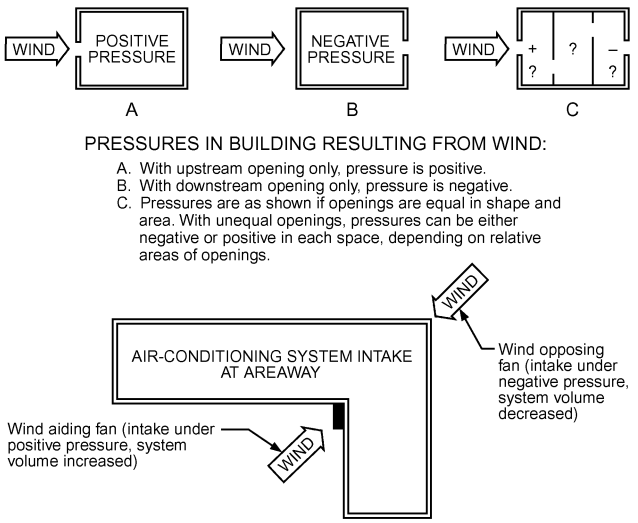

Fig. 11 Sensitivity of System Volume to Locations of Building Openings, Intakes, and Exhausts

and air-conditioning system operation. Wind can assist or hinder inlet and exhaust fans, depending on their positions on the building, but even in locations with a predominant wind direction, the ventilating system must perform adequately for all other directions. To avoid variable system flow rates, use Figures 4, 5, and 8 as a guide to placing inlets and exhausts in locations where surface pressure coefficients do not vary greatly with wind direction.

Airflow through a wall opening results from differential pressures, which may exceed 0.5 in. of water during high winds. Supply and exhaust systems, openings, dampers, louvers, doors, and windows make building flow conditions too complex for direct calculation. Iterative calculations are required because of the nonlinear dependence of volume flow rate on the differential pressure across an opening. Several multizone airflow models are available for these iterative calculations (Feustel and Dieris 1992; Walton and Dols 2005). Opening and closing of doors and windows by building occupants add further complications. In determining $C_{p(in\text{-}out)}$ from Equation (5), wind direction is more important than the position of an opening on a wall, as shown in Figures 4 and 5. Refer to Chapter 16 for details on wind effects on building ventilation, including natural and mechanical systems.

Cooling towers and similar equipment should be oriented to take advantage of prevailing wind directions, if possible, based on careful study of meteorological data and flow patterns on the building for the area and time of year.

Natural and Mechanical Ventilation

With natural ventilation, wind may augment, impede, or sometimes reverse the airflow through a building. For flat roof areas with large along-wind sides, wind can reattach to the roof downwind of the leading edge (see Figure 2). For peaked roofs, the upwind slope may be positively pressurized while the downwind slope may be negatively pressurized, as shown in Figure 8. Thus, any natural ventilation openings could see either a positive or negative pressure, dependent on wind speed and direction. Positive pressure existing where negative pressures were expected could reverse expected natural ventilation. These reversals can be avoided by using stacks, continuous roof ventilators, or other exhaust devices in which flow is augmented by wind.

Mechanical ventilation is also affected by wind conditions. A low-pressure wall exhaust fan (0.05 to 0.1 in. of water) can suffer drastic reduction in capacity. Flow can be reduced or reversed by wind pressure on upwind walls, or increased substantially when

subjected to negative pressure on the downwind wall. Side walls may be subjected to either positive or negative pressure, depending on wind direction. Clarke (1967), measuring medium-pressure air-conditioning systems (1 to 1.5 in. of water), found flow rate changes of 25% for wind blowing into intakes on an L-shaped building compared to wind blowing away from intakes. Such changes in flow rate can cause noise at supply outlets and drafts in the space served.

For mechanical systems, wind can be thought of as an additional pressure source in series with a system fan, either assisting or opposing it (Houlihan 1965). Where system stability is essential, supply and exhaust systems must be designed for high pressures (about 3 to 4 in. of water) or use devices to actively minimize unacceptable variations in flow rate. To conserve energy, the selected system pressure should be the minimum consistent with system needs.

Quantitative estimates of wind effects on a mechanical ventilation system can be made by using the pressure coefficients in Figures 4 to 9 to calculate wind pressure on air intakes and exhausts. A simple worst-case estimate is to assume a system with 100% makeup air supplied by a single intake and exhausted from a single outlet. The building is treated as a single zone, with an exhaust-only fan as shown in Figure 12. This overestimates the effect of wind on system volume flow.

Combining Equations (2) and (3), surface wind pressures at air intake and exhaust locations are

$$p_{s\ intake} = C_{p\ intake}\frac{\rho_a U_h^2}{2g_c} \tag{6}$$

$$p_{s\ exhaust} = C_{p\ exhaust}\frac{\rho_a U_h^2}{2g_c} \tag{7}$$

For the single-zone building shown in Figure 12, a worst-case estimate of wind effect neglects any flow resistance in the intake grill and duct, making interior building pressure $p_{interior}$ equal to outdoor wind pressure on the intake ($p_{interior} = p_{s\ intake}$). Then, with all system flow resistance assigned to the exhaust duct in Figure 12, and a pressure rise Δp_{fan} across the fan, pressure drop from outdoor intake to outdoor exhaust yields

$$(p_{s\ intake} - p_{s\ exhaust}) + \Delta p_{fan} = F_{sys}\frac{\rho Q^2}{A_L^2 g_c} \tag{8}$$

where F_{sys} is system flow resistance, A_L is flow leakage area, and Q is system volume flow rate. This result shows that, for the worst-case estimate, the wind-induced pressure difference simply adds to or subtracts from the fan pressure rise. With inlet and exhaust pressures from Equations (6) and (7), the effective fan pressure rise $\Delta p_{fan\ eff}$ is

$$\Delta p_{fan\ eff} = \Delta p_{fan} + \Delta p_{wind} \tag{9}$$

where

$$\Delta p_{wind} = (C_{p\ intake} - C_{p\ exhaust})\frac{\rho_a U_h^2}{2g_c} \tag{10}$$

The fan is wind-assisted when $C_{p\ intake} > C_{p\ exhaust}$ and wind-opposed when the wind direction changes, causing $C_{p\ intake} < C_{p\ exhaust}$. The effect of wind-assisted and wind-opposed pressure differences is illustrated in Figure 13.

Example 3. Make a worst-case estimate for the effect of wind on the supply fan for a low-rise building with height H = 50 ft, located in a city suburb. Use the hourly average wind speed that will be exceeded only 1% of the time and assume an annual hourly average speed of U_{annual} = 8 mph measured on a meteorological tower at height H_{met} = 33 ft at a nearby airport. Outdoor air density is $\rho_a = 0.075\ lb_m/ft^3$.

Solution: From Table 2, the wind speed exceeded only 1% of the hours each year is a factor of 2.5 ± 0.4 higher than the annual average of 8 mph, so the 1% maximum speed at the airport meteorological station is

$$U_{met} = 2.5 \times 8 = 20\ \text{mph}$$

From Example 1, building wind speed U_H is 18.2 mph.

A worst-case estimate of wind effect must assume intake and exhaust locations on the building that produce the largest difference ($C_{p\ intake} - C_{p\ exhaust}$) in Equations (9) and (10). From Figure 5, the largest difference occurs for the intake on the upwind wall AB and the exhaust on the downwind wall CD, with a wind angle $\theta_{AB} = 0°$. For this worst case, $C_{p\ intake} = +0.8$ on the upwind wall and $C_{p\ exhaust} = -0.43$ on the downwind wall. Using these coefficients in Equations (9) and (10) to evaluate effective fan pressure $\Delta p_{fan\ eff}$,

$$\Delta p_{fan\ eff} = \Delta p_{fan} + [0.8 - (-0.43)]\frac{0.075(23.2)^2}{2(32.2)}$$

$$= \Delta p_{fan} + 0.77\ lb_f/ft^2$$

This wind-assisted hourly averaged pressure is exceeded only 1% of the time (88 hours per year). When wind direction reverses, the outlet will be on the upwind wall and the inlet on the downwind wall, producing wind-opposed flow, changing the sign from +0.15

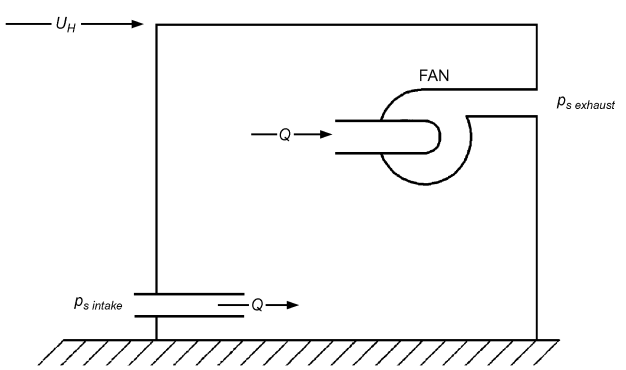

Fig. 12 Intake and Exhaust Pressures on Exhaust Fan in Single-Zone Building

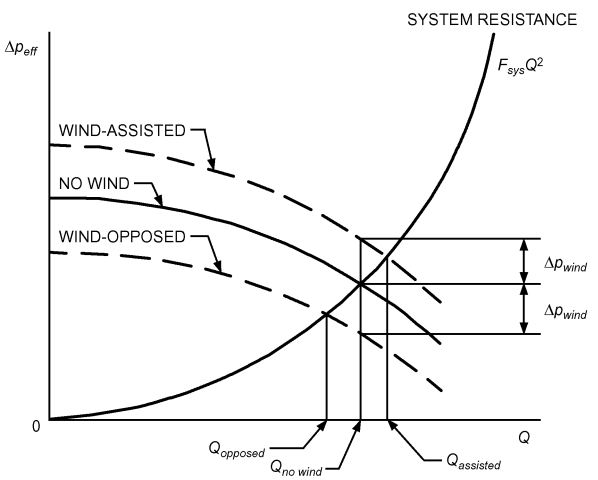

Fig. 13 Effect of Wind-Assisted and Wind-Opposed Flow

to –0.15 in. of water. The importance of these pressures depends on their size relative to the fan pressure rise Δp_{fan}, as shown in Figure 13.

Minimizing Wind Effect on System Volume

Wind effect can be reduced by careful selection of inlet and exhaust locations. Because wall surfaces are subject to a wide variety of positive and negative pressures, wall openings should be avoided when possible. When they are required, wall openings should be away from corners formed by building wings (see Figure 11). Mechanical ventilation systems should operate at a pressure high enough to minimize wind effect. Low-pressure systems and propeller exhaust fans should not be used with wall openings unless their ventilation rates are small or they are used in noncritical services (e.g., storage areas).

Although roof air intakes in flow recirculation zones best minimize wind effect on system flow rates, current and future air quality in these zones must be considered. These locations should be avoided if a contamination source exists or may be added in the future. The best area is near the middle of the roof, because the negative pressure there is small and least affected by changes in wind direction (see Figure 8). Avoid edges of the roof and walls, where large pressure fluctuations occur. Either vertical or horizontal (mushroom) openings can be used. On roofs with large areas, where intake may be outside the roof recirculation zone, mushroom or 180° gooseneck designs minimize impact pressure from wind flow. Vertical louvered openings or 135° goosenecks are undesirable for this purpose or for rain protection.

Heated air or contaminants should be exhausted vertically through stacks, above the roof recirculation zone. Horizontal, louvered (45° down), and 135° gooseneck discharges are undesirable, even for heat removal systems, because of their sensitivity to wind effects. A 180° gooseneck for hot-air systems may be undesirable because of air impingement on tar and felt roofs. Vertically discharging stacks in a recirculation region (except near a wall) have the advantage of being subjected only to negative pressure created by wind flow over the tip of the stack. See Chapter 44 of the 2007 *ASHRAE Handbook—HVAC Applications* for information on stack design.

Chemical Hood Operation

Wind effects can interfere with safe chemical hood operation. Supply volume variations can cause both disturbances at hood faces and a lack of adequate hood makeup air. Volume surges, caused by fluctuating wind pressures acting on the exhaust system, can cause momentary inadequate hood exhaust. If highly toxic contaminants are involved, surging is unacceptable. The system should be designed to eliminate this condition. On low-pressure exhaust systems, it is impossible to test the hoods under wind-induced, surging conditions. These systems should be tested during calm conditions for safe flow into the hood faces, and rechecked by smoke tests during high wind conditions. For more information on chemical hoods, see Chapter 14 of the 2007 *ASHRAE Handbook—HVAC Applications*. For more information on stack and intake design, see Chapter 44 of that volume.

BUILDING PRESSURE BALANCE AND INTERNAL FLOW CONTROL

Proper building pressure balance avoids flow conditions that make doors hard to open and cause drafts. In some cases (e.g., office buildings), pressure balance may be used to prevent confinement of contaminants to specific areas. In other cases (e.g., laboratories), the correct internal airflow is towards the contaminated area.

Pressure Balance

Although supply and exhaust systems in an internal area may be in nominal balance, wind can upset this balance, not only because of its effects on fan capacity but also by superimposing infiltrated or exfiltrated air (or both) on the area. These effects can make it impossible to control environmental conditions. Where building balance and minimum infiltration are important, consider the following:

- Design HVAC system with pressure adequate to minimize wind effects
- Include controls to regulate flow rate, pressure, or both
- Separate supply and exhaust systems to serve each building area requiring control or balance
- Use revolving or other self-closing doors or double-door air locks to noncontrolled adjacent areas, particularly outside doors
- Seal windows and other leakage sources
- Close natural ventilation openings

Internal Flow Control

Airflow direction is maintained by controlling pressure differentials between spaces. In a laboratory building, for example, peripheral rooms such as offices and conference rooms are kept at positive pressure, and laboratories at negative pressure, both with reference to corridor pressure. Pressure differentials between spaces are normally obtained by balancing supply system airflows in the spaces in conjunction with exhaust systems in the laboratories. Differential pressure instrumentation is normally used to control the airflow.

The pressure differential for a room adjacent to a corridor can be controlled using the corridor pressure as the reference. Outdoor pressure cannot usually control pressure differentials within internal spaces, even during periods of relatively constant wind velocity (wind-induced pressure). A single pressure sensor can measure the outside pressure at one point only and may not be representative of pressures elsewhere.

Airflow (or pressure) in corridors is sometimes controlled by an outdoor reference probe that senses static pressure at doorways and air intakes. The differential pressure measured between the corridor and the outside may then signal a controller to increase or decrease airflow to (or pressure in) the corridor. Unfortunately, it is difficult to locate an external probe where it will sense the proper external static pressure. High wind velocity and resulting pressure changes around entrances can cause great variations in pressure.

To measure ambient static pressure, the probe should be located where airflow streamlines are not affected by the building or nearby buildings. One possibility is at a height of 1.5R, as shown in Figure 1. However, this is usually not feasible. If an internal space is to be pressurized relative to ambient conditions, the pressure must be known on each exterior surface in contact with the space. For example, a room at the northeast corner of the building should be pressurized with respect to pressure on both the north and east building faces, and possibly the roof. In some cases, multiple probes on a single building face may be required. Figures 4 to 8 may be used as guides in locating external pressure probes. System volume and pressure control is described in Chapter 46 of the 2007 *ASHRAE Handbook—HVAC Applications*.

PHYSICAL AND COMPUTATIONAL MODELING

For many routine design applications, flow patterns and wind pressures can be estimated using the data and equations presented in the previous sections. Exhaust dilution for simple building geometries in homogeneous terrain environments (e.g., no larger buildings or terrain features nearby) can be estimated using the data and equations presented in the previous sections and in Chapter 44 of the 2007 *ASHRAE Handbook—HVAC Applications*. However, in critical applications, such as where health and safety are of concern, more accurate estimates may be required.

Computational Modeling

Computational fluid dynamics (CFD) models attempt to resolve airflow around buildings by solving the Navier-Stokes equations at

finite grid locations. CFD models are currently used to model internal flows (see Chapter 13), but are insufficient to accurately model atmospheric turbulence. According to Stathopoulos (2000, 2002), there is great potential for computational wind engineering (CWE), but the numerical wind tunnel "is still virtual rather than real." According to Murakami (2000), CWE has become a more popular tool, but results usually include numerical errors and prediction inaccuracies. Murakami also notes that, although issues remaining for improving CWE are not many, they are very difficult.

Different methods for predicting turbulent flow around buildings are described and compared in the following paragraphs.

Direct numerical simulation (DNS) directly resolves all the spatial and temporal scales in the flow based on the exact Navier-Stokes equations. This requires very extensive computational resources (runs lasting from several hours to days, depending on computer characteristics, power, and capacity) and can at present only be applied for flow in simple geometries and at low Reynolds numbers. For the complex, high-Re-number flows in wind engineering, application of DNS will not be possible in the foreseeable future.

Large eddy simulation (LES) is a simplified method in which the spatially filtered Navier-Stokes equations are solved. Turbulent structures larger than the filter (sometimes taken equal to the grid size) are explicitly solved, while those smaller than the filter are modeled (i.e., approximated) by a subfilter model. Information on filtering and subfilter models can be found in Ferzinger and Peric (2002), Geurts (2003), and Meyers et al. (2008).

In **Reynolds-averaged Navier-Stokes (RANS) simulation,** equations are obtained by averaging the Navier-Stokes equations (time-averaging if the flow is statistically steady or ensemble-averaging for time-dependent flows). With RANS, only the mean flow is solved, whereas all scales of turbulence must be modeled. Averaging generates additional unknowns for which turbulence models are required. Many turbulence models are available, but no single turbulence model is universally accepted as being the best for all types of applications.

In addition, hybrid RANS/LES approaches are available, in which **unsteady RANS (URANS)** is used near the wall, and LES in the rest of the flow field. This avoids the excessively high near-wall grid resolution required for application of LES near walls in high-Reynolds-number flow problems. An example of a hybrid RANS/LES approach is **detached eddy simulation (DES)**, as proposed by Spalart et al. (1997).

The statistically steady RANS method is the most widely applied and validated in CWE. It has been used for a wide range of building applications, including estimating pressure coefficients (Meroney et al. 2002; Murakami et al. 1992; Oliveira and Younis 2000; Richards and Hoxey 1992; Stathopoulos 1997; Stathopoulos and Zhou 1993); wind-driven rain (Blocken and Carmeliet 2002, 2004; Choi 1993, 1994; Tang and Davidson 2004); pollutant dispersion (Cowan et al. 1997; Dawson et al. 1991; Leitl et al. 1997; Li and Stathopoulos 1997; Meroney 2004; Meroney et al. 1999); pedestrian wind conditions (Blocken et al. 2008; Richards et al. 2002; Stathopoulos and Baskaran 1996; Yoshie et al. 2007); snow drift (Sundsbo 1998; Thiis 2000); and cooling tower drift (Meroney 2006, 2008). Although many past applications of RANS have been limited to isolated buildings or relatively simple building arrangements, large and sometimes very large discrepancies have been found in comparisons with wind tunnel and full-scale measurements. These are at least partly attributed to turbulence model limitations and to the statistically steady solution of flows that exhibit pronounced transient features, such as intermittent separation, recirculation zones, and vortex shedding. In addition, a wide range of other computational aspects can contribute to uncertainties and errors, divided by COST (2007) into two broad categories: physical and numerical. Physical modeling errors and uncertainties result from assumptions and approximations made in the mathematical description of the physical process. Examples are simplifications of the actual physical complexity (e.g., using RANS instead of DNS) and uncertainties and/or simplifications of the geometric and physical boundary conditions. Numerical errors and uncertainties are the result of the numerical solution of the mathematical model. Examples are computer programming errors, computer round-off errors, spatial and temporal discretization errors, and iterative convergence errors.

LES is a time-dependent approach in which more of the turbulence is resolved. It therefore has a larger potential to provide accurate results than statistically steady RANS simulations (Murakami et al. 1992; Tominaga et al. 1997). LES also provides more information about the flow, such as instantaneous and peak wind speeds, pressures, and pollutant concentrations. However, it requires considerably higher CPU times and memory than RANS. It also requires time- and space-resolved data as boundary conditions to properly simulate the inflow. Such experimental data are rarely available in practice (COST 2007). LES is also considered to require more experience for users to apply effectively than does RANS. These drawbacks imply that the practical application of CWE will continue to be based on statistically steady RANS for a considerable while.

Guidelines for using CFD have been developed and assembled to help users avoid, reduce, and estimate errors and uncertainties in applying CFD. ERCOFTAC (2000) provides extensive guidelines for industrial CFD applications, many of which are also applicable to CWE. COST (2007) assembled a comprehensive best-practice guideline document for CFD simulation of flows in the urban environment. Guidelines for application of CFD to pedestrian wind conditions around buildings and for predicting wind loads on buildings have been developed by the Architectural Institute of Japan and reported by Mochida et al. (2002), Tamura et al. (2008), Tominaga et al. (2008), and Yoshie et al. (2007). Other efforts have focused on specific problems, such as those encountered in simulating equilibrium atmospheric boundary layers in computational domains [e.g., Blocken et al. (2007a, 2007b); Hargreaves and Wright (2007); Richards and Hoxey (1993); Yang et al. (2008)]. Most of these guidelines apply to statistically steady RANS simulations.

Independent of whether RANS or LES is employed, evaluating the accuracy of CFD results by comparing them with wind tunnel or field experiments is very important because turbulence models are based on assumptions; no turbulence model is universally valid for all applications. Physical modeling therefore remains an indispensable tool in wind engineering.

Physical Modeling

Measurements on small-scale models in wind tunnels or water channels can provide information for design before construction. These measurements can also be used as an economical method of performance evaluation for existing facilities. Full-scale testing is not generally useful in the initial design phase because of the time and expense required to obtain meaningful information, but it is useful for verifying data derived from physical modeling and for planning remedial changes to improve existing facilities (Cochran 2006).

Detailed accounts of physical modeling, field measurements and applications, and engineering problems resulting from atmospheric flow around buildings are available in international journals, proceedings of conferences, and research reports on wind engineering (see the Bibliography).

The wind tunnel is the main tool used to assess and understand airflow around buildings. Water channels or tanks can also be used, but are more difficult to implement and give only qualitative results for some cases. Models of buildings, complexes, and the local surrounding topography are constructed and tested in a simulated turbulent atmospheric boundary layer. Airflow, wind pressures, snow loads, structural response, or pollutant concentrations can then be measured directly by properly scaling wind, building geometry, and

exhaust flow characteristics. Dagliesh (1975) and Petersen (1987a) found generally good agreement between the results of wind tunnel simulations and corresponding full-scale data. Cochran (1992) and Cochran and Cermak (1992) found good agreement between model- and full-scale measurements of low-rise architectural aerodynamics and cladding pressures, respectively. Stathopoulos et al. (1999, 2002, 2004) obtained good agreement between model- and full-scale measurements of the dispersion of gaseous pollutants from rooftop stacks on two different buildings in an urban environment.

Similarity Requirements

Physical modeling is most appropriate for applications involving small-scale atmospheric motions, such as recirculation of exhaust downwind of a laboratory, wind loads on structures, wind speeds around building clusters, snow loads on roofs, and airflow over hills or other terrain features. Winds associated with tornadoes, thunderstorms, and large-scale atmospheric motion cannot currently be physically modeled accurately.

Snyder (1981) gives guidelines for fluid modeling of atmospheric diffusion. This report contains explicit directions and should be used whenever designing wind tunnel studies to assess concentration levels of air pollutants. ASCE *Standard* 7, ASCE *Manual of Practice* 67 (ASCE 1999), and AWES *Quality Assurance Manual* (AWES 2001) also provide guidance when wind tunnels are used for evaluating wind effects on structures.

A complete and exact simulation of airflow over buildings and the resulting concentration or pressure distributions cannot be achieved in a physical model. However, this is not a serious limitation. Cermak (1971, 1975, 1976a, 1976b), Petersen (1987a, 1987b), and Snyder (1981) found that transport and dispersion of laboratory exhaust can be modeled accurately if the following criteria are met in the model and full scale:

1. Match exhaust velocity to wind speed ratios, V_e/U_H.
2. Match exhaust to ambient air density ratios, ρ_e/ρ_a.
3. Match exhaust Froude numbers. $Fr^2 = \rho_a V_e^2/[(\rho_e - \rho_a)gd]$, where d is effective exhaust stack diameter.
4. Ensure fully turbulent stack gas flow by ensuring stack flow Reynolds number ($Re_s = V_e d/\nu$) is greater than 2000 [where ν is the kinematic viscosity of ambient (outdoor) air], or by placing an obstruction inside the stack to enhance turbulence.
5. Ensure fully turbulent wind flow.
6. Scale all dimensions and roughness by a common factor.
7. Match atmospheric stability by the bulk Richardson number (Cermak 1975). For most applications related to airflow around buildings, neutral stratification is assumed, and no Richardson number matching is required.
8. Match mean velocity and turbulence distributions in the wind.
9. Ensure building wind Reynolds number ($Re_b = U_H R/\nu$) is greater than 11,000 for sharp-edged structures, or greater than 90,000 for round-edged structures.
10. Ensure less than 5% blockage of wind tunnel cross section.

For wind speeds, flow patterns, or pressure distributions around buildings, only conditions 5 to 10 are necessary. Usually, each wind tunnel study requires a detailed assessment to determine the appropriate parameters to match in the model and full scale.

In wind tunnel simulations of exhaust gas recirculation, buoyancy of the exhaust gas (condition 3) is often not modeled. This allows using a high wind tunnel speed or a smaller model to achieve high enough Reynolds numbers (conditions 4, 5, and 9). Neglecting buoyancy is justified if the density of building exhaust air is within 10% of the ambient (outdoor) air. Also, critical minimum dilution D_{crit} occurs generally at wind speeds high enough to produce a well-mixed, neutrally stable atmosphere, allowing stability matching (condition 7) to be neglected (see Chapter 44 of the 2007 *ASHRAE Handbook—HVAC Applications* for discussion of D_{crit}). However, in some cases and depending on emission sources, calm conditions may produce critical dilution. Nevertheless, omission of conditions 3 and 7 simplifies the test procedure considerably, reducing both testing time and cost.

Buoyancy should be properly simulated for high-temperature exhausts such as boilers and diesel generators. Equality of model and prototype Froude numbers (condition 3) requires tunnel speeds of less than 100 fpm for testing. However, greater tunnel speeds may be needed to meet the minimum building Reynolds number requirement (condition 4).

Wind Simulation Facilities

Boundary layer wind tunnels are required for conducting most wind studies. The wind tunnel test section should be long enough to establish, upwind of the model building, a deep boundary layer that slowly changes with downwind distance.

Other important wind tunnel characteristics include width and height of the test section, range of wind speeds, roof adjustability, and temperature control. Larger models can be used in tunnels that are wider and taller, which, in turn, give better measurement resolution. Model blockage effects can be minimized by an adjustable roof height. Temperature control of the tunnel surface and airflow is required when atmospheric conditions other than neutral stability are to be simulated. Boundary layer characteristics appropriate for the site are established by using roughness elements on the tunnel floor that produce mean velocity, turbulence intensity profiles, and spectra characteristic of full scale.

Water can also be used for the modeling fluid if an appropriate flow facility is available. Flow facilities may be in the form of a tunnel, tank, or open channel. Water tanks with a free surface ranging in size up to that of a wind tunnel test section have been used by towing a model (upside down) through the nonflowing fluid. Stable stratification can be obtained by adding a salt solution. This technique does not allow development of a boundary layer and therefore yields only approximate, qualitative information on flow around buildings. Water channels can be designed to develop thick turbulent boundary layers similar to those developed in the wind tunnel. One advantage of such a flow system is ease of flow visualization, but this is offset by a greater difficulty in developing the correct turbulence structure and the measurement of flow variables and concentrations.

Designing Model Test Programs

The first step in planning a test program is selecting the model length scale. This choice depends on cross-sectional dimensions of the test section, dimensions of the buildings to be modeled, and/or topographic features and thickness of the simulated atmospheric boundary layer. Typical geometric scales range from about 120:1 to 1000:1.

Because a large model is desirable to meet minimum Reynolds and Froude number requirements, a wide test section is advantageous. In general, the model at any section should be small compared to the test section area so that blockage is less than 5% (Melbourne 1982).

The test program must include specifications of the meteorological variables to be considered (e.g., wind direction, wind speed, thermal stability). Data taken at the nearest meteorological station should be reviewed to obtain a realistic assessment of wind climate for a particular site. Ordinarily, local winds around a building, pressures, and/or concentrations are measured for 16 wind directions (e.g., 22.5° intervals). This is easily accomplished by mounting the building model and its nearby surroundings on a turntable. More than 16 wind directions are required for highly toxic exhausts or for finding peak fluctuating pressures on a building. If only local wind information and pressures are of interest, testing at one wind speed with neutral stability is sufficient.

SYMBOLS

a = exponent in power law wind speed profile for local building terrain, Equation (4) and Table 1, dimensionless
A_L = flow leakage area, Equation (8), ft^2
a_{met} = exponent a for the meteorological station, Equation (4) and Table 1, dimensionless
B_L = larger of two upwind building face dimensions H and W, Equation (1), ft
B_s = smaller of two upwind building face dimensions H and W, Equation (1), ft
C_p = local wind pressure coefficient for building surface, Equation (3), dimensionless
$C_{p\,in}$ = internal wind-induced pressure coefficient, Equation (5), dimensionless
$C_{p(in\text{-}out)}$ = difference between outdoor and indoor pressure coefficients, Equation (5), dimensionless
C_s = surface-averaged pressure coefficient, Figure 6, dimensionless
d = effective stack diameter, ft
D_{crit} = critical dilution factor at roof level for uncapped vertical exhaust at critical wind speed (see Chapter 44 of the 2007 *ASHRAE Handbook—HVAC Applications*), dimensionless
Fr = Froude number, dimensionless
F_{sys} = system flow resistance, Equation (8), dimensionless
g = acceleration of gravity, 32.2 ft/s^2
g_c = gravitational proportionality constant, Equations (2), (6), (7), (10), 32.2 ft·lb$_m$/lb$_f$·s^2
H = wall height above ground on upwind building face, Equation (4) and Figure 1, ft
H_c = maximum height above roof level of upwind roof edge flow recirculation zone, Figures 1 and 3, ft
H_{met} = height of anemometer at meteorological station, Equation (4), ft
h_s = exhaust stack height (typically above roof unless otherwise specified, ft (see Figure 3, and Chapter 44 in the 2007 *ASHRAE Handbook—HVAC Applications*)
L = length of building in wind direction, Figures 1 and 2, ft
L_c = length of upwind roof edge recirculation zone, Figure 3, ft
L_r = length of flow recirculation zone behind rooftop obstacle or building, Figures 1 and 3, ft
p_s = wind pressure difference between exterior building surface and local ambient (outdoor) atmospheric pressure at same elevation in undisturbed approach wind, Equation (3), lb$_f$/ft^2
p_v = wind velocity pressure at roof level, Equation (2), lb$_f$/ft^2
Q = volumetric flow rate, Equation (8), cfm
R = scaling length for roof flow patterns, Equation (1), ft
Re$_b$ = building Reynolds number, dimensionless
Re$_s$ = stack flow Reynolds number, dimensionless
S = stretched-string distance; shortest distance from exhaust to intake over obstacles and along building surface, ft (see Figure 3, and Chapter 44 in the 2007 *ASHRAE Handbook—HVAC Applications*)
U_{annual} = annual average of hourly wind speeds U_{met}, Table 2, mph
U_H = mean wind speed at height H of upwind wall in undisturbed flow approaching building, Equation (2) and Figures 1, 2, and 3, mph
U_{met} = meteorological station hourly wind speed, measured at height H_{met} above ground in smooth terrain, Equation (4) and Table 2, mph
V_e = exhaust face velocity, mph
W = width of upwind building face, Figure 2, ft

Greek

δ = fully developed atmospheric boundary layer thickness, Equation (4) and Table 1, ft
δ_{met} = atmospheric boundary layer thickness at meteorological station, Equation (4) and Table 1, ft
Δp_{fan} = pressure rise across fan, Equation (8), psi
$\Delta p_{fan\,eff}$ = effective pressure rise across fan, Equation (9), psi
Δp_{wind} = wind-induced pressure, Equations (9) and (10), psi
θ = angle between perpendicular line from upwind building face and wind direction, Figures 4 to 7, degrees
ν = kinematic viscosity of ambient (outdoor) air, ft^2/s
ρ_a = ambient (outdoor) air density, Equation (2), lb$_m$/ft^3
ρ_e = density of exhaust gas mixture, lb$_m$/ft^3

REFERENCES

Akins, R.E., J.A. Peterka, and J.E. Cermak. 1979. Averaged pressure coefficients for rectangular buildings. *Wind Engineering: Proceedings of the Fifth International Conference*, vol. 7, pp. 369-380.

ASCE. 2006. Minimum design loads for buildings and other structures. *Standard* ASCE/SEI 7-05. American Society of Civil Engineers, New York.

ASCE. 1999. Wind tunnel studies of buildings and structures. *ASCE Manuals and Reports on Engineering Practice* 67. American Society of Civil Engineers, New York.

AWES. 2001. *Quality assurance manual—Wind engineering studies of buildings*. AWES-QAM-1-2001. The Australasian Wind Engineering Society, Melbourne.

Bailey, P.A. and K.C.S. Kwok. 1985. Interference excitation of twin fall buildings. *Wind Engineering and Industrial Aerodynamics* 21:323-338.

Bair, F.E. 1992. *The weather almanac*, 6th ed. Gale Research, Inc., Detroit.

Blocken, B. and J. Carmeliet. 2002. Spatial and temporal distribution of driving rain on a low-rise building. *Wind and Structures* 5(5):441-462.

Blocken, B. and J. Carmeliet. 2004. A review of wind-driven rain research in building science. *Journal of Wind Engineering and Industrial Aerodynamics* 92(13):1079-1130.

Blocken, B., J. Carmeliet, and T. Stathopoulos. 2007a. CFD evaluation of the wind speed conditions in passages between buildings—Effect of wall-function roughness modifications on the atmospheric boundary layer flow. *Journal of Wind Engineering and Industrial Aerodynamics* 95(9-11):941-962.

Blocken, B., T. Stathopoulos, and J. Carmeliet. 2007b. CFD simulation of the atmospheric boundary layer: Wall function problems. *Atmospheric Environment* 41(2):238-252.

Blocken, B., P. Moonen, T. Stathopoulos, and J. Carmeliet. 2008. A numerical study on the existence of the Venturi-effect in passages between perpendicular buildings. *Journal of Engineering Mechanics—ASCE* 134(12).

Cermak, J.E. 1971. Laboratory simulation of the atmospheric boundary layer. *AIAA Journal* 9(9):1746.

Cermak, J.E. 1975. Applications of fluid mechanics to wind engineering. *Journal of Fluid Engineering, Transactions of ASME* 97:9.

Cermak, J.E. 1976a. Nature of airflow around buildings. *ASHRAE Transactions* 82(1):1044-1060.

Cermak, J.E. 1976b. Aerodynamics of buildings. *Annual Review of Fluid Mechanics* 8:75.

Choi, E.C.C. 1993. Simulation of wind-driven rain around a building. *Journal of Wind Engineering and Industrial Aerodynamics* 46/47:721-729.

Choi, E.C.C. 1994. Determination of wind-driven rain intensity on building faces. *Journal of Wind Engineering and Industrial Aerodynamics* 51:55-69.

Clarke, J.H. 1967. Airflow around buildings. *Heating, Piping and Air Conditioning* 39(5):145.

Cochran, L.S. 1992. Low-rise architectural aerodynamics: The Texas Tech University experimental building. *Architectural Science Review* 35(4): 131-136.

Cochran, L.S. 2006. State of the art review of wind tunnels and physical modeling to obtain structural loads and cladding pressures. *Architectural Science Review* 50(1):7-16.

Cochran, L.S. and J.E. Cermak. 1992. Full and model scale cladding pressures on the Texas Tech University experimental building. *Journal of Wind Engineering and Industrial Aerodynamics* 41-44:1589-1600.

Cochran, L.S. and E.C. English. 1997. Reduction of wind loads by architectural features. *Architectural Science Review* 40(3):79-87.

Cochran, L.S., J.A. Peterka, and R.J. Derickson. 1999. Roof surface wind speed distributions on low-rise buildings. *Architectural Science Review* 42(3):151-160.

COST. 2007. *Best practice guideline for the CFD simulation of flows in the urban environment. COST action 732: Quality assurance and improvement of microscale meteorological models.* J. Franke, A. Hellsten, H. Schlünzen, and B. Carissimo, eds. European Cooperation in the field of Scientific and Technical Research, Brussels.

Cowan, I.R., I.P. Castro, and A.G. Robins. 1997. Numerical considerations for simulations of flow and dispersion around buildings. *Journal of Wind Engineering and Industrial Aerodynamics* 67/68:535-545.

Dagliesh, W.A. 1975. Comparison of model/full-scale wind pressures on a high-rise building. *Journal of Industrial Aerodynamics* 1:55-66.

Davenport, A.G. and H.Y.L. Hui. 1982. *External and internal wind pressures on cladding of buildings.* Boundary Layer Wind Tunnel Laboratory, University of Western Ontario, London, Canada. BLWT-820133.

Dawson, P., D.E. Stock, and B. Lamb. 1991. The numerical simulation of airflow and dispersion in three-dimensional atmospheric recirculation zones. *Journal of Applied Meteorology* 30:1005-1024.

Deaves, D.M. 1981. Computations of wind flow over changes in surface roughness. *Journal of Wind Engineering and Industrial Aerodynamics* 7:65-94.

Deaves, D.M. and R.I. Harris. 1978. A mathematical model of the structure of strong winds. *Report* 76. Construction Industry Research and Information Association (U.K.).

DOC. 1968. *Climatic atlas of the United States*. U.S. Department of Commerce, Washington, D.C.

English, E.C. and F.R. Fricke. 1997. The interference index and its prediction using a neural network analysis of wind tunnel data. *Fourth Asia-Pacific Symposium on Wind Engineering*, APSOWE IV University of Queensland, pp. 363-366.

ERCOFTAC. 2000. *Special interest group on quality and trust in industrial CFD: Best practice guidelines.* M. Casey, and T. Wintergerste, eds. European Research Community on Flow, Turbulence and Combustion, Brussels.

Ferziger, J.H. and M. Peric. 2002. *Computational methods for fluid mechanics.* Springer.

Feustel, H.E. and J. Dieris. 1992. A survey of airflow models for multizone buildings. *Energy and Buildings* 18:79-100.

Geurts, B.J. 2003. *Elements of direct and large-eddy simulation*. Edwards Publishing, Las Vegas.

Hargreaves, D.M. and N.G. Wright. 2007. On the use of the *k*-ε model in commercial CFD software to model the neutral atmospheric boundary layer. *Journal of Wind Engineering and Industrial Aerodynamics* 95(5):355-369.

Holmes, J.D. 1983. *Wind loads on low rise buildings—A review.* Commonwealth Scientific and Industrial Research Organisation (CSIRO), Division of Building Research, Australia.

Holmes, J.D. 1986. *Wind loads on low-rise buildings: The structural and environmental effects of wind on buildings and structures*, Chapter 12. Faculty of Engineering, Monash University, Melbourne, Australia.

Hosker, R.P. 1984. Flow and diffusion near obstacles. In *Atmospheric science and power production*. U.S. Department of Energy DOE/TIC-27601 (DE 84005177).

Hosker, R.P. 1985. Flow around isolated structures and building clusters: A review. *ASHRAE Transactions* 91(2b):1671-1692.

Houlihan, T.F. 1965. Effects of relative wind on supply air systems. *ASHRAE Journal* 7(7):28.

Khanduri, A.C., T. Stathopoulos, and C. Bédard. 1998. Wind-induced interference effects on buildings—A review of the state-of-the-art. *Engineering Structures* 20(7):617-630.

Leitl, B.M., P. Kastner-Klein, M. Rau, and R.N. Meroney. 1997. Concentration and flow distributions in the vicinity of U-shaped buildings: Wind-tunnel and computational data. *Journal of Wind Engineering and Industrial Aerodynamics* 67/68:745-755.

Li, Y. and T. Stathopoulos. 1997. Numerical evaluation of wind-induced dispersion of pollutants around a building. *Journal of Wind Engineering and Industrial Aerodynamics* 67/68:757-766.

Melbourne, W.H. 1979. Turbulence effects on maximum surface pressures; A mechanism and possibility of reduction. *Proceedings of the Fifth International Conference on Wind Engineering*, J.E. Cermak, ed., pp. 541-551.

Melbourne, W.H. 1982. Wind tunnel blockage effects and corrections. *Proceedings of the International Workshop on Wind Tunnel Modeling Criteria and Techniques in Civil Engineering Applications*, T.A. Reinhold, ed., pp. 197-216.

Meroney, R.N. 2004. *Wind tunnel and numerical simulation of pollution dispersion: A hybrid approach*. Invited lecture at Croucher Advanced Study Institute on Wind Tunnel Modeling, Hong Kong University of Science and Technology, 6-10 December, 2004. Available at www.engr.colostate.edu/~meroney/projects/ASI Crocher Paper Final.pdf.

Meroney, R.N. 2006. CFD prediction of cooling tower drift. *Journal of Wind Engineering and Industrial Aerodynamics* 94(6):463-490.

Meroney, R.N. 2008. Protocol for CFD prediction of cooling-tower drift in an urban environment. *Journal of Wind Engineering and Industrial Aerodynamics* 96(10-11):1789-1804.

Meroney, R.N., B.M. Leitl, S. Rafailidis, and M. Schatzmann. 1999. Wind-tunnel and numerical modeling of flow and dispersion about several building shapes. *Journal of Wind Engineering and Industrial Aerodynamics* 81(1-3):333-345.

Meroney, R.N., C.W. Letchford, and P.P. Sarkar. 2002. Comparison of numerical and wind tunnel simulation of wind loads on smooth, rough and dual domes immersed in a boundary layer. *Wind and Structures* 5(2-4):347-358.

Meyers, J., B.J. Geurts, and P. Sagaut, eds. 2008. Quality and reliability of large-eddy simulations. *ERCOFTAC Series*, vol. 12. European Research Community on Flow, Turbulence, and Combustion, Lausanne, Switzerland, and Springer, Netherlands.

Mochida, A., Y. Tominaga, S. Murakami, R. Yoshie, T. Ishihara, and R. Ooka. 2002. Comparison of various *k*-ε models and DSM to flow around a high rise building—Report of AIJ cooperative project for CFD prediction of wind environment. *Wind and Structures* 5(2-4):227-244.

Murakami, S. 2000. Overview of CWE 2000. International Symposium on Computational Wind Engineering. PF Consultants.

Murakami, S., A. Mochida, Y. Hayashi, and S. Sakamoto. 1992. Numerical study on velocity-pressure field and wind forces for bluff bodies by *k*-ε, ASM and LES. *Journal of Wind Engineering and Industrial Aerodynamics* 41-44:2841-2852.

NCDC. Updated periodically. *International station meteorological climatic summary* (CD-ROM). National Climatic Data Center, Asheville, NC. Published jointly with U.S. Air Force and U.S. Navy.

Oliveira, P.J. and B.A. Younis. 2000. On the prediction of turbulent flows around full-scale buildings. *Journal of Wind Engineering and Industrial Aerodynamics* 86(2-3):203-220.

Petersen, R.L. 1987a. Wind tunnel investigation of the effect of platform-type structures on dispersion of effluents from short stacks. *Journal of Air Pollution Control Association* 36:1347-1352.

Petersen, R.L. 1987b. Designing building exhausts to achieve acceptable concentrations of toxic effluent. *ASHRAE Transactions* 93(2):2165-2185.

Richards, P.J. and R.P. Hoxey. 1992. Computational and wind tunnel modelling of mean wind loads on the Silsoe structures building. *Journal of Wind Engineering and Industrial Aerodynamics* 43(1-3):1641-1652.

Richards, P.J. and R.P. Hoxey. 1993. Appropriate boundary conditions for computational wind engineering models using the *k*-ε turbulence model. *Journal of Wind Engineering and Industrial Aerodynamics* 46/47:145-153.

Richards, P.J., G.D. Mallison, D. McMillan, and Y.F. Li. 2002. Pedestrian level wind speeds in downtown Auckland. *Wind and Structures* 5(2-4): 151-164.

SA/SNZ. 2002. Structural design actions—Part 2: Wind actions. *Standard* AS/NZS 1170.2:2002. Standards Australia International Ltd., Sydney.

Saunders, J.W. and W.H. Melbourne. 1979. Buffeting effect of upwind buildings. *Fifth International Conference on Wind Engineering.* Pergamon Press, pp. 593-606.

Sherman, M.H. and D.T. Grimsrud. 1980. The measurement of infiltration using fan pressurization and weather data. *Report* LBL-10852. Lawrence Berkeley Laboratory, University of California.

Snyder, W.H. 1981. Guideline for fluid modeling of atmospheric diffusion. Environmental Protection Agency *Report* EPA-600/881-009.

Spalart, P., W.-H. Jou, M. Strelets, and S. Allmaras. 1997. Comments on the feasibility of LES for wings and on the hybrid RANS/LES approach. *Advances in DNS/LES, 1st AFOSR International Conference on DNS/LES*, Greden Press.

Stathopoulos, T. 1997. Computational wind engineering: Past achievements and future challenges. *Journal of Wind Engineering and Industrial Aerodynamics* 67/68:509-532.

Stathopoulos, T. 2000. The numerical wind tunnel for industrial aerodynamics: Real or virtual in the new millennium? Third International Symposium on Computational Wind Engineering. PF Consultants.

Stathopoulos, T. 2002. The numerical wind tunnel for industrial aerodynamics: Real or virtual in the new millennium? *Wind and Structures* 5(2-4):193-208.

Stathopoulos, T. and B.A. Baskaran. 1996. Computer simulation of wind environmental conditions around buildings. *Engineering Structures* 18 (11):876-885.

Stathopoulos, T. and Y.S. Zhou. 1993. Numerical simulation of wind-induced pressures on buildings of various geometries. *Journal of Wind Engineering and Industrial Aerodynamics* 46/47:419-430.

Stathopoulos, T., L. Lazure, and P. Saathoff. 1999. Tracer gas investigation of reingestion of building exhaust in an urban environment. IRSST *Report* R-213, Robert-Sauvé Institute of Occupational Health and Safety Research (IRSST), Montreal, Canada.

Stathopoulos, T., L. Lazure, P. Saathoff, and X. Wei. 2002. Dilution of exhaust from a rooftop stack on a cubical building in an urban environment. *Atmospheric Environment* 36:4577-4591.

Stathopoulos, T., L. Lazure, P. Saathoff, and A. Gupta. 2004. The effect of stack height, stack location and rooftop structures on air intake contamination. A laboratory and full-scale study. IRSST *Report* R-392. Robert-Sauvé Institute of Occupational Health and Safety Research (IRSST), Montreal, Canada.

Sundsbo, P.A. 1998. Numerical simulations of wind deflection fins to control snow accumulation in building steps. *Journal of Wind Engineering and Industrial Aerodynamics* 74-76:543-552.

Swami, M.V. and S. Chandra. 1987. Procedures for calculating natural ventilation airflow rates in buildings. *Final Report* FSEC-CR-163-86. Florida Solar Energy Center, Cape Canaveral.

Tamura, T., K. Nozawa, and K. Kondo. 2008 AIJ guide for numerical prediction of wind loads on buildings. *Journal of Wind Engineering and Industrial Aerodynamics* 96(10-11):1974-1984.

Tang, W. and C.I. Davidson. 2004. Erosion of limestone building surfaces caused by wind-driven rain: 2. Numerical modeling. *Atmospheric Environment* 38(33):5601-5609.

Thiis, T.K. 2000. A comparison of numerical simulations and full-scale measurements of snowdrifts around buildings. *Wind and Structures* 3(2): 73-81.

Tominaga, Y., S. Murakami, and A. Mochida. 1997. CFD prediction of gaseous diffusion around a cubic model using a dynamic mixed SGS model based on composite grid technique. *Journal of Wind Engineering and Industrial Aerodynamics* 67/68: 827-841.

Tominaga, Y., A. Mochida, R. Yoshie, H. Kataoka, T. Nozu, M. Yoshikawa, and T. Shirasawa. 2008. AIJ guidelines for practical applications of CFD to pedestrian wind environment around buildings. *Journal of Wind Engineering and Industrial Aerodynamics* 96(10-11):1749-1761.

Walker, I.S., D.J. Wilson, and T.W. Forest. 1996. Wind shadow model for air infiltration sheltering by upwind obstacles. *International Journal of HVAC&R Research* (now *HVAC&R Research*) 2(4):265-283.

Walton, G.N. and W.S. Dols. 2005. *CONTAM 2.4 user guide and program documentation*. NISTIR 7251. National Institute of Standards and Technology, Gaithersburg, Maryland.

Wilson, D.J. 1979. Flow patterns over flat roofed buildings and application to exhaust stack design. *ASHRAE Transactions* 85(2):284-295.

Yang, W., Y. Quan, X. Jin, Y. Tamura, and M. Gu. 2008. Influences of equilibrium atmosphere boundary layer and turbulence parameters on wind load distributions of low-rise buildings. *Journal of Wind Engineering and Industrial Aerodynamics* 96(10-11):2080-2092.

Yoshie, R., A. Mochida, Y. Tominaga, H. Kataoka, K. Harimoto, T. Nozu, and T. Shirasawa. 2007. Cooperative project for CFD prediction of pedestrian wind environment in the architectural institute of Japan. *Journal of Wind Engineering and Industrial Aerodynamics* 95(9-11):1551-1578.

BIBLIOGRAPHY

AIHA. 2003. Laboratory ventilation. ANSI/AIHA *Standard* Z9.5-2003. American Industrial Hygiene Association, Fairfax, VA.

ASCE. 1987. Wind tunnel model studies of building and structures. *ASCE Manuals and Reports on Engineering Practice* 67. American Society of Civil Engineers, New York.

Cermak, J.E. 1977. Wind-tunnel testing of structures. *Journal of the Engineering Mechanics Division*, ASCE 103, EM6:1125.

Cermak, J.E., ed. 1979. Wind engineering. *Wind Engineering: Proceedings of the Fifth International Conference*, Colorado State University, Fort Collins, CO. Pergamon Press, New York.

Clarke, J.H. 1965. The design and location of building inlets and outlets to minimize wind effect and building reentry of exhaust fumes. *Journal of American Industrial Hygiene Association* 26:242.

CWE. 1993. *Proceedings of the 1st International Symposium on Computational Wind Engineering*, Tokyo, Japan. Elsevier.

CWE. 1997. *Proceedings of the 2nd International Symposium on Computational Wind Engineering*, Colorado State University, Fort Collins. Elsevier.

CWE. 2000. *Proceedings of the 3rd International Symposium on Computational Wind Engineering*. PF Consultants.

CWE. 2006. *Proceedings of the 4th International Symposium on Computational Wind Engineering,* Yokohama, Japan. Elsevier.

Defant, F. 1951. Local winds. In *Compendium of meteorology*, pp. 655-672. American Meteorology Society, Boston.

Elliot, W.P. 1958. The growth of the atmospheric internal boundary layer. *Transactions of the American Geophysical Union* 39:1048-1054.

ESDU. 1990. Strong winds in the atmospheric boundary layer. Part 1: Mean hourly wind speeds, pp. 15-17. *Engineering Science Data Unit*, Item 82-26, London.

Geiger, R. 1966. *The climate near the ground*. Harvard University, Cambridge.

Houghton, E.L. and N.B. Carruthers. 1976. *Wind forces on buildings and structures: An introduction*. Edward Arnold, London.

Landsberg, H. 1981. *The urban climate*. Academic Press, New York.

Meroney, R.N. and B. Bienkiewicz, eds. 1997. *Computational wind engineering 2*. Elsevier, Amsterdam.

Panofsky, H.A. and J.A. Dutton. 1984. *Atmospheric turbulence: Models and methods for engineering applications*. John Wiley & Sons, New York.

Simiu, V. and R. Scanlan. 1986. *Wind effects on structures: An introduction to wind engineering*, 2nd ed. Wiley Interscience, New York.

WERC. 1985. *Proceedings of the 5th U.S. National Conference on Wind Engineering*, 6-8 November, Texas Tech University, Lubbock. Mehta, K.C. and R.A. Dillingham, eds. Wind Engineering Research Center, Lubbock.